

## Quantum spin Hall states in graphene interacting with WS<sub>2</sub> or WSe<sub>2</sub>

T. P. Kaloni, L. Kou, T. Frauenheim, and U. Schwingenschlögl

Citation: *Applied Physics Letters* **105**, 233112 (2014); doi: 10.1063/1.4903895

View online: <http://dx.doi.org/10.1063/1.4903895>

View Table of Contents: <http://scitation.aip.org/content/aip/journal/apl/105/23?ver=pdfcov>

Published by the [AIP Publishing](#)

---

### Articles you may be interested in

[Quantum valley Hall states and topological transitions in Pt\(Ni, Pd\)-decorated silicene: A first-principles study](#)

*J. Chem. Phys.* **141**, 244701 (2014); 10.1063/1.4904285

[Topological phase transition and quantum spin Hall state in TlBiS<sub>2</sub>](#)

*J. Appl. Phys.* **116**, 033704 (2014); 10.1063/1.4890226

[First-principles study of graphene adsorbed on WS<sub>2</sub> monolayer](#)

*J. Appl. Phys.* **114**, 183709 (2013); 10.1063/1.4829483

[Quantum spin Hall effect induced by electric field in silicene](#)

*Appl. Phys. Lett.* **102**, 043113 (2013); 10.1063/1.4790147

[Transport in quantum spin Hall phase of graphene nanoribbons](#)

*J. Appl. Phys.* **112**, 063713 (2012); 10.1063/1.4754427

---

The advertisement features a photograph of the Model PS-100 cryogenic probe station, which is a complex piece of scientific equipment with various mechanical components and a probe. The background is a gradient of blue. The text is arranged around the image: the model name and description on the left, the company logo in the center, and a slogan on the right.

**Model PS-100**  
Tabletop Cryogenic  
Probe Station

The logo for Lake Shore CRYOTRONICS consists of a stylized blue and white square icon to the left of the company name 'Lake Shore' in a large, white, sans-serif font, with 'CRYOTRONICS' in a smaller, white, sans-serif font below it.

*An affordable solution for  
a wide range of research*

## Quantum spin Hall states in graphene interacting with WS<sub>2</sub> or WSe<sub>2</sub>

T. P. Kaloni,<sup>1</sup> L. Kou,<sup>2</sup> T. Frauenheim,<sup>2</sup> and U. Schwingenschlög<sup>1,a)</sup>

<sup>1</sup>Physical Science and Engineering Division, KAUST, Thuwal 23955-6900, Kingdom of Saudi Arabia

<sup>2</sup>Bremen Center for Computational Materials Science, University of Bremen, Am Falturm 1, 28359 Bremen, Germany

(Received 24 September 2014; accepted 30 November 2014; published online 10 December 2014)

In the framework of first-principles calculations, we investigate the structural and electronic properties of graphene in contact with as well as sandwiched between WS<sub>2</sub> and WSe<sub>2</sub> monolayers. We report the modification of the band characteristics due to the interaction at the interface and demonstrate that the presence of the dichalcogenide results in quantum spin Hall states in the absence of a magnetic field. © 2014 AIP Publishing LLC. [<http://dx.doi.org/10.1063/1.4903895>]

Research on freestanding graphene today appears to have reached a peak, mainly because the material is rather difficult to be utilized in electronic devices due to limitations in high quality mass production. Thus, interest is shifting to hybrid systems with other two-dimensional materials, both for application purposes and to create opportunities to better understand basic physical and chemical phenomena.<sup>1,2</sup> Heterostructures of semiconducting MoS<sub>2</sub> and graphene already have been demonstrated, showing potential particularly in data storage.<sup>3</sup> Moreover, the joint two-dimensional nature of the two components can be utilized for fabricating large scale flexible nanoelectronic devices. For example, a new generation of field effect transistors based on heterostructures of WS<sub>2</sub> and graphene on transparent and flexible substrates has shown a promising performance.<sup>4</sup>

Two-dimensional topological insulators in a quantum spin Hall (QSH) state have metallic edges that sustain dissipationless current flow.<sup>5,6</sup> For freestanding graphene, this effect has been predicted by Kane and Mele using an analytical model.<sup>7</sup> Since the energy gap is tiny ( $\sim 10^{-3}$  meV) due to the small intrinsic spin-orbit coupling (SOC),<sup>8</sup> realization of a QSH state, however, is difficult. Various ideas for an enhancement have been put forward, all based on proximity to areas in that the electrons are subject to strong SOC, including heavy atom deposition,<sup>9</sup> H adsorption,<sup>10</sup> and heterostructures with MoTe<sub>2</sub> and Bi<sub>2</sub>Te<sub>3</sub>.<sup>11</sup>

Experimental realization of a QSH state in the topological insulator HgTe<sup>5</sup> has initiated efforts on many other materials. Recently, experiments have demonstrated that graphene in a strong magnetic field supports a QSH state, which is interesting for quantum circuits.<sup>12</sup> However, the difficulties coming along with large magnetic fields<sup>13</sup> call for alternative approaches. In this work, we propose hybrid structures that host a QSH state in the absence of a magnetic field. Specifically, we employ density functional theory (including van der Waals corrections) to study the following structures: (a) graphene on WS<sub>2</sub> or WSe<sub>2</sub> and (b) graphene sandwiched between WS<sub>2</sub> or WSe<sub>2</sub>. Our results prevail that the SOC in graphene is enhanced and that QSH states are realized in the absence of a magnetic field.

The heterostructures are constructed by joining a  $4 \times 4 \times 1$  supercell of graphene with  $3 \times 3 \times 1$  supercells of the

dichalcogenides. A vacuum layer of at least 15 Å thickness guarantees that there is no artificial interaction perpendicular to the two-dimensional system due to the periodic boundary conditions. For the structural relaxation, we employ the Quantum-ESPRESSO code,<sup>14</sup> using the generalized gradient approximation (GGA) and including van der Waals forces via Grimme's approach.<sup>15</sup> The atomic positions are optimized until all forces have converged to less than 0.005 eV/Å. The electronic structure calculations are then performed using the Vienna *Ab-initio* Simulation Package<sup>16</sup> both with pure GGA and including the SOC. A plane wave cutoff energy of 450 eV and a Monkhorst-Pack  $16 \times 16 \times 1$  k-mesh are employed.

The systems under consideration are illustrated in Fig. 1. The lattice parameters of the graphene (9.98 Å) and WS<sub>2</sub> supercells (9.57 Å) give rise to a lattice mismatch of 2.7%. The distance between the two subsystems converges to  $d = 3.41$  Å, see Table I, which is a typical value for graphene on a semiconducting substrate. We observe no modification of the C–C bond lengths, whereas the W–S bond lengths (2.45–2.46 Å) are modified as compared to pristine WS<sub>2</sub> (2.39 Å (Ref. 17)) because of the lattice relaxation. We find  $d = 3.42$  Å for graphene on WSe<sub>2</sub> with a C–C bond length of 1.42 Å, which is the value of pristine graphene. The W–Se bond length (2.52–2.53 Å) is almost the same as in pristine WSe<sub>2</sub> (2.52 Å (Ref. 17)). Moreover, we obtain  $d = 3.40$  Å and  $d = 3.42$  Å for graphene sandwiched between

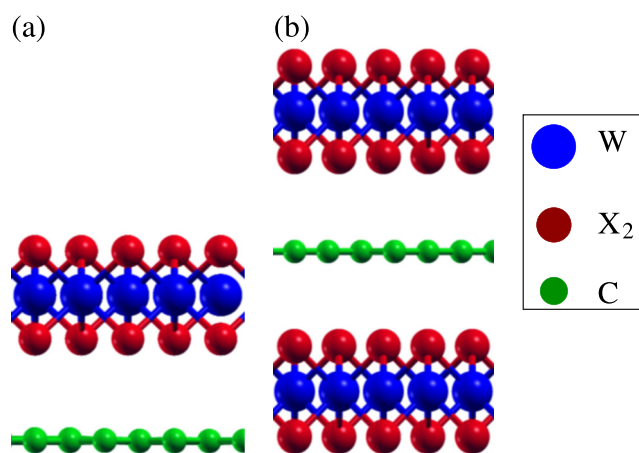


FIG. 1. (a) Graphene in contact with one dichalcogenide monolayer. (b) Graphene sandwiched between two dichalcogenide monolayers.

<sup>a)</sup>Email: udo.schwingenschlogl@kaust.edu.sa. Tel.: +966-544700080.

TABLE I. Distance between the subsystems ( $d$ ), binding energy per C atom ( $E_b$ ), band gap ( $E_g$ ), valence band splitting ( $\Delta_v$ ), and conduction band splitting ( $\Delta_c$ ).

System	GGA			GGA + SOC		
	$d$ (Å)	$E_b$ (meV)	$E_g$ (meV)	$E_g$ (meV)	$\Delta_v$ (meV)	$\Delta_c$ (meV)
Graphene/WS <sub>2</sub>	3.41	53	1	1	33	33
WS <sub>2</sub> /graphene/WS <sub>2</sub>	3.40	51	0	1	92	99
Graphene/WSe <sub>2</sub>	3.42	54	4	1	145	132
WSe <sub>2</sub> /graphene/WSe <sub>2</sub>	3.42	52	3	1	149	153

WS<sub>2</sub> and WSe<sub>2</sub> layers, respectively, whereas the other structural parameters are the same as for the simple contacts.

While graphene is a zero-gap semiconductor, WS<sub>2</sub> has a direct band gap of 1.30–1.35 eV.<sup>18</sup> The structural and electronic properties have been studied extensively, see Ref. 19 and the references therein, as WS<sub>2</sub> is widely utilized for  $n/p$ -doped field effect transistors, for example.<sup>20</sup> Experimentally, synthesis and characterization of graphene on WS<sub>2</sub> have been reported in Ref. 4, claiming that a device based on this system can operate at room temperature with good current modulating capacity. We show in Fig. 2(a) the band structure obtained for graphene on WS<sub>2</sub> without SOC, demonstrating some interaction between the two subsystems, though without chemical bonding. The binding energy

$$E_{\text{binding}} = E_{\text{graphene/WS}_2} - E_{\text{WS}_2} - E_{\text{graphene}}$$

( $E_{\text{graphene/WS}_2}$ ,  $E_{\text{WS}_2}$ , and  $E_{\text{graphene}}$  are the total energies of the hybrid structure, WS<sub>2</sub>, and graphene, respectively) amounts to 53 meV per C atom, in agreement with Ref. 21. Due to this weak interaction (physisorption), a small band gap of about 1 meV is obtained, see the zoomed view in Fig. 2(a), with degeneracy of the K and K' points.

When the SOC is switched on in the calculation, the spin degeneracy of the bands is lifted, resulting in valence and conduction band splittings of 33 meV, see Table I, with a non-trivial band gap of 1 meV, see the right hand side of Fig.

2(a). A similar behavior has been observed for graphene on Bi<sub>2</sub>Te<sub>3</sub> and MoTe<sub>2</sub>.<sup>11</sup> The characteristic shape of the bands near the Fermi level signifies a QSH phase (band inversion under preserved time-reversal symmetry), similar to the observations in InAs/GaSb.<sup>22</sup> It should be noted that the bands above and below the Fermi level have opposite spin in agreement with the signature of the QSH phase. A similar picture appears in germanene nanorods embedded in fully H-passivated germanene<sup>23</sup> and in two-dimensional Sn,<sup>24</sup> for which the gap can be strongly enhanced by the application of strain such that devices can operate at room temperature.

In Fig. 2(b), we present results for graphene sandwiched between WS<sub>2</sub> layers. We find essentially no band gap without SOC, reflecting a very weak interaction between the subsystems, and again a non-trivial band gap of 1 meV when the SOC is taken into account. The shape of the band structure reflects a QSH state also in this case. Larger valence and conduction band splittings of 92 meV and 99 meV, respectively, are achieved because here two WS<sub>2</sub> layers are attached to the graphene sheet and influence its electronic states, see Table I. The situation is similar to the 70 meV band splitting of graphene in contact with the (111) surface of BiFe<sub>3</sub> (which is magnetic and thus hosts a quantum anomalous Hall effect<sup>25</sup>).

We next study hybrid systems with monolayer WSe<sub>2</sub>, which is a semiconductor with a band gap of 1.65 eV.<sup>26</sup> The binding energy of graphene on WSe<sub>2</sub> (54 meV) turns out to be similar to the WS<sub>2</sub> case and also the band gap remains small (4 meV). Again, according to Fig. 3(a), the spin degeneracy at the K and K' points is lifted under inclusion of the SOC. The band structure qualitatively reflects the same characteristics as demonstrated for WS<sub>2</sub> in Fig. 2(a). While the size of the non-trivial band gap remains 1 meV, the valence and conduction band splittings are enhanced to 145 meV and 132 meV, respectively. This finding agrees with the fact that the band splitting due to SOC is about 50 meV larger in bulk WSe<sub>2</sub> than in bulk WS<sub>2</sub>.<sup>27,28</sup> For graphene sandwiched between WSe<sub>2</sub> layers, we find a similar band gap and under SOC an enhancement of the valence and conduction band splittings to 149 meV and 153 meV, respectively, compare

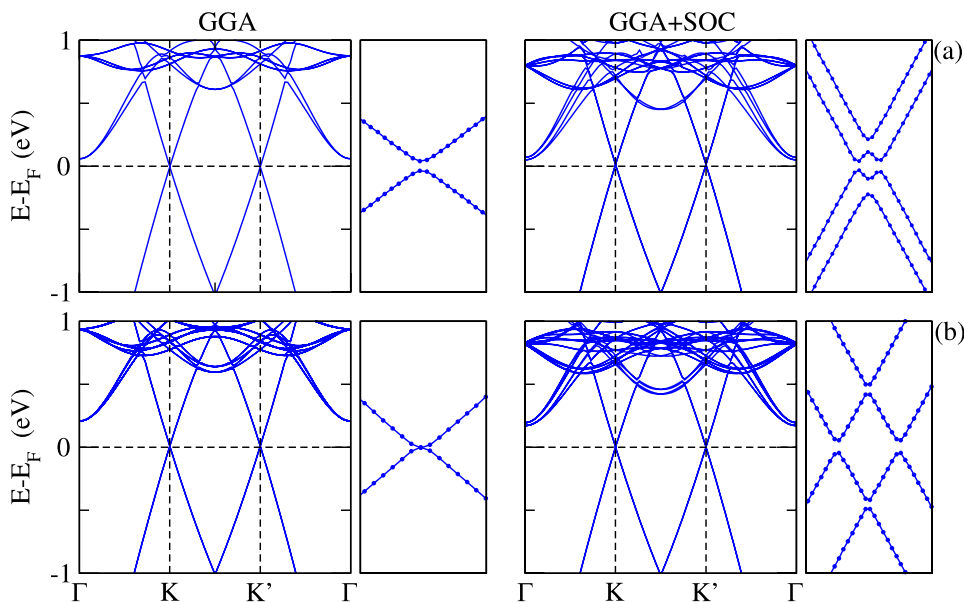


FIG. 2. GGA and GGA + SOC band structures for (a) graphene on WS<sub>2</sub> and (b) graphene sandwiched between WS<sub>2</sub> layers. Zoomed views of the K point are shown to clarify the band splitting.

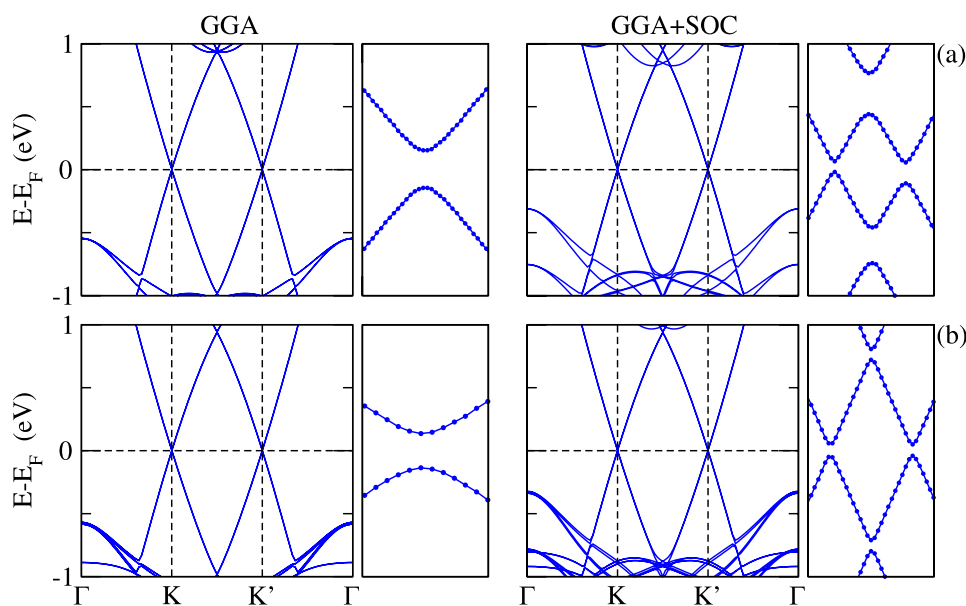


FIG. 3. GGA and GGA + SOC band structures for (a) graphene on  $\text{WSe}_2$  and (b) graphene sandwiched between  $\text{WSe}_2$  layers. Zoomed views of the K point are shown to clarify the band splitting.

Fig. 3(b) with Fig. 2(b), as to be expected from our previous discussion. In the  $\text{WSe}_2$  systems, the QSH effect therefore is significantly more pronounced than in the  $\text{WS}_2$  systems.

Based on first-principles calculations, we have investigated the structural and electronic properties of hybrid systems consisting of graphene and  $\text{WS}_2$  or  $\text{WSe}_2$ . The SOC leads to band inversion at the K/K' points and a surprisingly stable non-trivial band gap of 1 meV, reflecting QSH states for all four hybrid systems under investigation. By the preserved time-reversal symmetry combined with enhancement of the effective SOC in graphene, these systems are able to realize topological phases. Usually a strong magnetic field is needed to achieve a QSH state in graphene,<sup>12</sup> while we propose systems in that this state appears in the absence of a magnetic field.

Research reported in this publication was supported by the King Abdullah University of Science and Technology (KAUST).

<sup>1</sup>K. S. Novoselov, V. I. Fal'ko, L. Colombo, P. R. Gellert, M. G. Schwab, and K. Kim, *Nature* **490**, 192 (2012).

<sup>2</sup>A. K. Geim, *Nature* **499**, 419 (2013).

<sup>3</sup>S. Bertolazzi, D. Krasnozhan, and A. Kis, *ACS Nano* **7**, 3246 (2013).

<sup>4</sup>T. Georgiou, R. Jalil, B. D. Belle, L. Britnell, R. V. Gorbachev, S. V. Morozov, Y.-J. Kim, A. Gholinia, S. J. Haigh, O. Makarovskiy, L. Eaves, L. A. Ponomarenko, A. K. Geim, K. S. Novoselov, and A. Mishchenko, *Nat. Nanotechnol.* **8**, 100 (2013).

<sup>5</sup>B. A. Bernevig, T. L. Hughes, and S. C. Zhang, *Science* **314**, 1757 (2006).

<sup>6</sup>A. Roth, C. Brüne, H. Buhmann, L. W. Molenkamp, J. Mauciejko, X. L. Qi, and S. C. Zhang, *Science* **325**, 294 (2009).

<sup>7</sup>C. L. Kane and E. J. Mele, *Phys. Rev. Lett.* **95**, 226801 (2005).

<sup>8</sup>Y. Yao, F. Ye, X. L. Qi, S. C. Zhang, and Z. Fang, *Phys. Rev. B* **75**, 041401 (2007).

<sup>9</sup>C. Weeks, J. Hu, J. Alicea, M. Franz, and R. Wu, *Phys. Rev. X* **1**, 021001 (2011).

<sup>10</sup>J. Balakrishnan, G. K. W. Koon, M. Jaiswal, A. H. Castro Neto, and B. Özyilmaz, *Nat. Phys.* **9**, 284 (2013).

<sup>11</sup>L. Kou, F. Hu, B. Yan, T. Wehling, C. Felser, T. Frauenheim, and C. Chen, e-print [arXiv:1309.6653v1](https://arxiv.org/abs/1309.6653v1).

<sup>12</sup>A. F. Young, J. D. Sanchez-Yamagishi, B. Hunt, S. H. Choi, K. Watanabe, T. Taniguchi, R. C. Ashoori, and P. Jarillo-Herrero, *Nature* **505**, 528 (2014).

<sup>13</sup>W. Bao, Z. Zhao, H. Zhang, G. Liu, P. Kratz, L. Jing, J. Velasco, D. Smirnov, and C. N. Lau, *Phys. Rev. Lett.* **105**, 246601 (2010).

<sup>14</sup>P. Giannozzi, S. Baroni, N. Bonini, M. Calandra, R. Car, C. Cavazzoni, D. Ceresoli, G. L. Chiarotti, M. Cococcioni, I. Dabo, A. Dal Corso, S. de Gironcoli, S. Fabris, G. Fratesi, R. Gebauer, U. Gerstmann, C. Gougoussis, A. Kokalj, M. Lazzeri, L. Martin-Samos, N. Marzari, F. Mauri, R. Mazzarello, S. Paolini, A. Pasquarello, L. Paulatto, C. Sbraccia, S. Scandolo, G. Sclauzero, A. P. Seitsonen, A. Smogunov, P. Umari, and R. M. Wentzcovitch, *J. Phys.: Condens. Matter* **21**, 395502 (2009).

<sup>15</sup>S. Grimme, *J. Comput. Chem.* **27**, 1787 (2006).

<sup>16</sup>G. Kresse and J. Furthmüller, *Comput. Mater. Sci.* **6**, 15 (1996).

<sup>17</sup>W. S. Yun, S. W. Han, S. C. Hong, I. G. Kim, and J. D. Lee, *Phys. Rev. B* **85**, 033305 (2012).

<sup>18</sup>D. Braga, I. G. Lezama, H. Berger, and A. F. Morpurgo, *Nano Lett.* **12**, 5218 (2012).

<sup>19</sup>W. Ki, X.-Y. Huang, J. Li, D. L. Young, and Y. Zhang, *J. Mater. Res.* **22**, 1390 (2007).

<sup>20</sup>A. Matthaus, A. Ennaoui, S. Fiechter, S. Tiefenbacher, T. Kiesewetter, K. Diesner, I. Sieber, W. Jaegermann, T. Tsirlina, and R. Tenne, *J. Electrochem. Soc.* **144**, 1013 (1997).

<sup>21</sup>S.-S. Li and C.-W. Zhang, *J. Appl. Phys.* **114**, 183709 (2013).

<sup>22</sup>C. Liu, T. L. Hughes, X.-L. Qi, K. Wang, and S.-C. Zhang, *Phys. Rev. Lett.* **100**, 236601 (2008).

<sup>23</sup>L. Seixas, J. E. Padilha, and A. Fazzio, *Phys. Rev. B* **89**, 195403 (2014).

<sup>24</sup>Y. Xu, B. Yan, H.-J. Zhang, J. Wang, G. Xu, P. Tang, W. Duan, and S.-C. Zhang, *Phys. Rev. Lett.* **111**, 136804 (2013).

<sup>25</sup>Z. Qiao, W. Ren, H. Chen, L. Bellaïche, Z. Zhang, A. H. MacDonald, and Q. Niu, *Phys. Rev. Lett.* **112**, 116404 (2014).

<sup>26</sup>C.-H. Chang, X. Fan, S.-H. Lin, and J.-L. Kuo, *Phys. Rev. B* **88**, 195420 (2013).

<sup>27</sup>A. Ramasubramaniam, *Phys. Rev. B* **86**, 115409 (2012).

<sup>28</sup>B. Amin, T. P. Kaloni, and U. Schwingenschlögl, *RSC Adv.* **4**, 34561 (2014).